Taylor & Francis
Taylor & Francis Group

Numerical Heat Transfer, Part A: Applications
An International Journal of Computation and Methodology

ISSN: (Print) (Online) Journal homepage: https://www.tandfonline.com/loi/unht20

Numerical analysis of fluid type and flow mass rate on logarithmic temperature difference and heat transfer coefficient of double pipe heat exchanger

Savaş Evran & Mustafa Kurt

To cite this article: Savaş Evran & Mustafa Kurt (2023): Numerical analysis of fluid type and flow mass rate on logarithmic temperature difference and heat transfer coefficient of double pipe heat exchanger, Numerical Heat Transfer, Part A: Applications, DOI: 10.1080/10407782.2023.2252173

To link to this article: https://doi.org/10.1080/10407782.2023.2252173

NUMERICAL HEAT TRANSFER, PART A: APPLICATIONS
https://doi.org/10.1080/10407782.2023.2252173

Taylor & Francis
Taylor & Francis Group

Numerical analysis of fluid type and flow mass rate on logarithmic temperature difference and heat transfer coefficient of double pipe heat exchanger

Savaş Evran[a] and Mustafa Kurt[b]

[a]Department of Jewelry and Jewelry Design, Marmara University, Faculty of Applied Sciences, Istanbul, Turkey; [b]Department of Mechanical Engineering, Marmara University, Faculty of Technology, Istanbul, Turkey

ABSTRACT

This CFD and statistical article aims to evaluate the impact of fluid type and flow mass rate on the log-mean temperature difference (ΔT_{LM}) and the heat transfer coefficient (U_{shell}) in a double tube heat exchanger (DPHEX) using computational fluid dynamics (CFD) and statistical analysis. ANSYS Fluent software was utilized to conduct CFD calculations. CFD analyses were implemented using Taguchi L8 orthogonal array containing two variables such as the fluid types and the flow mass rates. The levels of fluid types were considered as water-liquid, ethylene-glycol, engine-oil, and benzene-liquid. The levels of fluid types were decided as 1.1 kg/s to 1.5 kg/s. To determine the optimal levels of variables and their impacts on the ΔT_{LM} and U_{shell} in DPHEX, analysis of Signal to Noise (S/N) ratio was employed. Analysis of Variance (ANOVA) was also utilized to decide the effective variables and their percentage contribution rates on the outcomes. The CFD result obtained using the optimum levels of variables were compared with Taguchi estimation result. According to the study, the highest effects were obtained using ethylene-glycol, engine-oil, water-liquid, and benzene-liquid on the highest log-mean temperature difference values, respectively. In addition, the highest heat transfer coefficient values were found utilizing water-liquid, benzene-liquid, ethylene-glycol, and engine-oil, respectively. Increasing flow mass rate from 1.1 kg/s to 1.5 kg/s causes an increase in both outcomes. The study provides a reference for resolving issues that may arise in the production of experimental DPHEXs.

ARTICLE HISTORY
Received 15 May 2023
Revised 25 July 2023
Accepted 22 August 2023

KEYWORDS
ANOVA; CFD; heat exchanger; Taguchi method; temperature

1. Introduction

In the energy sector, DPHEXs can play a crucial role by facilitating effective heat transfer, which may be of paramount importance. With their compact design and versatility, they can be highly suitable for different applications, ranging from power generation to industrial processes. These heat exchangers have the potential to enhance thermal efficiency by enabling the transfer of heat between different fluids, thus potentially optimizing overall system performance and minimizing energy wastage. Analysis of DPHEXs with ANSYS Fluent is important because it allows engineers to simulate and optimize their thermal performance. By using CFD simulations, engineers can examine the flow and heat transfer activities of DPHEXs under various conditions, and identify potential issues such as fouling, pressure drop, or temperature gradients. This type of analysis is crucial for ensuring the safe and efficient operation of heat exchangers, decreasing costs, and

CONTACT Savaş Evran savas.evran@marmara.edu.tr Department of Jewelry and Jewelry Design, Marmara University, Faculty of Applied Sciences, Istanbul, Turkey.

improving overall system performance. Therefore, many heat exchangers dealing with CFD analysis have been studied in the literature. Mukesh Kumar and Chandrasekar [1] performed thermal performance analysis of heat exchanger made from helical tube utilizing nanofluid containing nanoparticles with different volume ratios and ANSYS Fluent software and compared CFD outcomes utilizing the experimental outcomes. Shahril et al. [2] carried out the thermal performance analysis based on numerical methods using heat exchangers and visually examined the temperature distributions in the heat exchangers based on the numerical results. Thondiyil and Kizhakke Kodakkattu [3] analyzed the thermal performance of the heat exchangers utilizing the numerical and Taguchi approach. They also evaluated the impact of some parts of the heat exchangers on the analyses. In the calculations, 64 CFD calculations were performed. Vivekanandan et al. [4] analyzed the heat exchanger numerically and experimentally, and as a result of the study, they found a successful numbness among the experimental data and the numerical data. Wang et al. [5] evaluated the analysis of the heat exchangers using numerical and statistical methods and completed the calculations based on the Taguchi orthogonal array. In addition, they evaluated the effect ratios of the factors and discussed with the help of ANOVA. Zheng et al. [6] investigated the effect of nanoparticle on heat exchangers and also evaluated the effect of different nanoparticles. Li et al. [7] found that using twisted oval tubes as inner tubes in double tube heat exchangers significantly enhances shell-side heat transport performance, increasing it by 24.0–39.0%. Rajeh et al. [8] investigated the coaxial ground heat exchanger (GHE) established superior heat transfer performance in accordance with a conventional double U-tube GHE, with lower thermal resistance and pressure drop. Additionally, replacing the double U-tube GHE with the coaxial GHE offered the most cost-effective alternative, resulting in reduced energy consumption and total annual cost. Luo and Song [9] discussed the thermohydraulic performance of a novel design for a DPHEX, which involved twisted annuli between two counter-twisted oval tubes. Obtained outcomes indicated that the twisted annulus generated strong secondary flow, significantly enhancing heat transfer. Correlations were proposed for heat transfer and friction factors as functions of Re number, twist ratio, and aspect ratio. Qi et al. [10] examined the thermal performance and pressure drop using nanofluids including nanoparticles in DPHEXs. The outcomes of the study display that the use of nanofluids meaningfully enhances the heat transfer rate while also increasing the pressure drop. Moya-Rico et al. [11] examined the impact of various configurations of twisted tape elements on the thermo-hydraulic performance of a smooth DPHEX using a high-viscosity fluid simulant. Their 320 experimental tests showed reasonable agreement between the obtained correlations and experimental data, with minimal deviations in heat transfer rate (less than 9.5%) and friction factor (less than 15%). Baker et al. [12] aim to develop a fast and accurate 3-D estimation algorithm for the thermal performance of BHE in a ground-source heat pump installation, considering the complex characteristics of BHE installations with various length scales. Asinari [13] analyzed mesh definition in accordance with difficult heat exchangers, distinguishing grid generation and cell discretization to improve accuracy. They modify the surrounded quadratic finite element for finned surfaces, making it intrinsically conservative, and suggest using FEM only for high Biot number finned surfaces due to increased computational time. Khanlari et al. [14] evaluated the experimental and mathematical simulations of a corrugated chevron plate heat exchanger (PHE) to predict heat transfer characteristics and fluid performance. Also, they highlighted that employing CFD could effectively develop the PHE's performance, and the incorporation of nanofluid resulted in an improved average heat transfer rate within the heat exchanger. Apart from these studies, the Taguchi approach has been used in many studies [15–20]. As it can be understood from the literature review, there are many numerical studies performed using CFD analysis. However, studies including statistical technique and CFD are very limited. In the CFD and statistical study, ΔT_{LM} and U_{shell} in the DPHEX was investigated utilizing the Taguchi and CFD approaches.

2. Materials and methods

DPHEXs are generally utilized in various engineering processes for transferring heat among two fluids. Materials and fluids can play a crucial case in the scheme and performance of double tube heat exchangers. Materials used for constructing double tube heat exchangers can be able to withstand high temperatures, pressure, and corrosive fluids. Metals used for the inner and outer tube usually are materials such as copper, stainless steel, and titanium. These materials are chosen based on their thermal conductivity, corrosion resistance, and mechanical strength. High viscosity or dense fluids may result in a higher pressure drop across the exchanger, reducing its efficiency. In this study, steel material was used in the design of the heat exchangers. To decide the impact of each fluid on ΔT_{LM} and U_{shell}, fluids with different properties were selected. The properties of these materials and liquids are illustrated in Table 1 [21].

Steel is a common material used for constructing these heat exchangers due to its excellent mechanical strength and resistance to high temperatures and corrosive fluids. For the inner tube, materials such as copper, stainless steel, or titanium may be used depending on the specific application requirements. Water-liquid, engine-oil, and ethylene-glycol are fluids with different thermal properties that can be used in double tube heat exchangers. Water, for example, has high thermal conductivity and is often used as a heat transfer fluid in cooling systems. Engine oil, on the other hand, is a specialized fluid used in automotive engines that can also be used in heat exchangers to transfer heat from the engine to the surrounding environment. Ethylene-glycol is commonly used as a coolant in refrigeration systems. Choosing the right materials and fluids based on the specific application requirements is essential for achieving optimal efficiency and durability.

3. CFD analysis

To optimize the performance of DPHEXs, numerical simulations using ANSYS Fluent are commonly employed. By solving the governing equations of fluid dynamics, CFD models can accurately predict the velocity calculation, pressure chance, and temperature profile for flow inside the heat exchanger. In CFD analysis, near-wall treatment is important to accurately model the fluid flow and heat transfer performance of DPHEX. The near-wall area is where the fluid flow is most complex due to the collaboration among the liquid and the heat exchanger wall. The Realizable k-epsilon model, with its improved turbulence modeling and near-wall treatment, is particularly effective in simulating the liquid flow and heat transfer behavior in the region. Constant parameters used in CFD analyzes are demonstrated in Table 2.

In the study, a DPHEX was used. The inner tube carries the hot fluid, whereas the outer tube carries the cold fluid. Water was used as the cold fluid. Four different fluids types for hot fluid were considered. Thus, the influence of each fluid on ΔT_{LM} and U_{shell} was evaluated. Flow was evaluated as counter flow. This creates a temperature gradient across the exchanger, which can allow for efficient heat transfer among the two fluids. Dimensions of DPHEX are presented in Figure 1.

In CFD investigation, the realizable k-epsilon approach is utilized as viscous model. Also, Realizable k-epsilon model may be described to be a turbulence model with two equations, which predicts the kinetic energy for turbulent and its dissipation rate to simulate the turbulent flow

Table 1. Material Properties of metal and fluids [21].

Properties	Unit	Steel	Water	Ethylene-glycol	Engine-oil	Benzene-liquid
Density	kg/m^3	8030	998.2	1111.4	889	875
Specific heat	J/kg-K	502.48	4182	2415	1845	1759
Thermal conductivity	W/m-K	16.27	0.6	0.252	0.145	0.159
Viscosity	kg/m-s	–	0.001003	0.0157	1.06	0.000589

Table 2. Constant parameters for CFD analysis.

Viscous model	Realizable k-epsilon
Near-wall treatment	Enhanced wall functions
Turbulent kinetic energy	Second order upwind
Specific dissipation rate	Second order upwind
Energy	Second order upwind
Initialization method	Hybrid initialization
Number of iterations	1000
Wall thickness	1 mm
Inner pipe diameter (Tube-Side)	36 mm
Outer pipe diameter (Shell-Side)	80 mm
Fluid type	Liquid
Flow mass rate for hot fluid in inner pipe	1 kg/s
Temperature of fluid in inner pipe	345 K
Fluid type in outer pipe	Water
Material of pipes	Steel

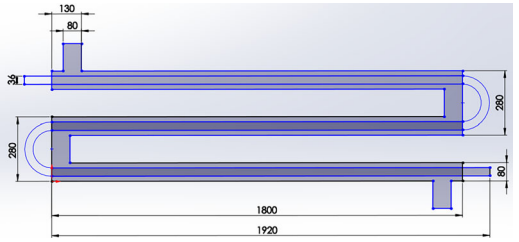

Figure 1. Dimensions for DPHEX.

within DPHEX. The continuity, momentum, stress tensor and energy equations used for ANSYS Fluent software are described below, respectively [22]:

$$\frac{\partial \rho}{\partial t} + \nabla\left(\rho \vec{v}\right) = S_m \tag{1}$$

$$\frac{\partial}{\partial t}\left(\rho \vec{v}\right) + \nabla\left(\rho \vec{v}\,\vec{v}\right) = -\nabla p + \nabla \bar{\bar{\tau}} + \rho \vec{g} + \vec{F} \tag{2}$$

$$\bar{\bar{\tau}} = \mu\left[\left(\nabla \vec{v} + \nabla \vec{v}^{T}\right) - \frac{2}{3}\nabla \vec{v} I\right] \tag{3}$$

$$\frac{\partial(\rho E)}{\partial t} + \nabla.\left[\vec{v}(\rho E + p)\right] = \nabla.\left(k_{eff}\nabla T - \sum_j h_j \vec{J}_j + \left(\bar{\bar{\tau}}_{eff}.\vec{v}\right)\right) + S_h \tag{4}$$

where, $\vec{v}$, S_m, $\bar{\bar{\tau}}$, $\vec{g}$, $\vec{F}$, E, k_{eff}, $\vec{J}_j$, $\bar{\bar{\tau}}_{eff}.\vec{v}$, S_h express the velocity vector, source term, stress tensor, acceleration due to gravity, external force, energy, effective conductivity, diffusion flux, viscous dispersion, source term of energy, respectively. In addition to these equations, in the analysis of DPHEX at different temperatures, the following equation for ΔT_{LM} are also solved [23, 24]:

$$\Delta T_{LM} = \frac{(\Delta T_1 - \Delta T_2)}{In\left(\frac{\Delta T_1}{\Delta T_2}\right)} \tag{5}$$

where, ΔT_1 and ΔT_2 present the temperature differences occurred between the two liquids for the inflow and outflow of DPHEX. ΔT_1 and ΔT_2 are calculated as follows, respectively.

$$\Delta T_1 = T_{inlet,\ tube} - T_{outlet,shell} \tag{6}$$

$$\Delta T_2 = T_{outlet,pipe} - T_{inlet,shell} \tag{7}$$

Heat transfer coefficient for shell in DPHEX is solved by the following equation [25].

$$U = \frac{Q}{A\Delta T_{LM}} \tag{8}$$

$$Q = \dot{m_{cw}} C_{p,cw}(\Delta T_{cw}) \tag{9}$$

in which, U denotes the heat transfer coefficient for shell in DPHEX. $\dot{m_{cw}}$, $C_{p,cw}$, ΔT_{cw} denote the mass flow rate of liquid in shell, the heat capacity of liquid in shell, and the temperature difference of water in shell, respectively. The Realizable k-epsilon (RKE) turbulence model takes into account the impacts of turbulence, which can have a vital influence on the heat transfer process. By accurately predicting the turbulence characteristics of the fluid flow, the RKE model can provide more accurate predictions of the overall performance of the heat exchanger. Equations governing the transportation of variables in the Realizable k-epsilon model [22]:

$$\frac{\partial}{\partial t}(\rho k) + \frac{\partial}{\partial x_j}(\rho k u_j) = \frac{\partial}{\partial x_j}\left[\left(\mu + \frac{\mu_t}{\sigma_k}\right)\frac{\partial k}{\partial x_j}\right] + G_k + G_b - \rho\epsilon - Y_M + S_k \tag{10}$$

$$\frac{\partial}{\partial t}(\rho\epsilon) + \frac{\partial}{\partial x_j}(\rho\epsilon u_j) = \frac{\partial}{\partial x_j}\left[\left(\mu + \frac{\mu_t}{\sigma_\epsilon}\right)\frac{\partial \epsilon}{\partial x_j}\right] + \rho C_1 S_\epsilon - \rho C_2 \frac{\epsilon^2}{k + \sqrt{\upsilon\epsilon}} + C_{1\epsilon}\frac{\epsilon}{k}C_{3\epsilon}G_b + S_\epsilon \tag{11}$$

$$C_1 = \max\left[0.43,\ \frac{\eta}{\eta + 5}\right],\ \eta = S\frac{k}{\epsilon},\ S = \sqrt{2S_{ij}S_{ij}} \tag{12}$$

in which, G_k, G_b, and Y_M correspond to the following phenomena in relation to turbulence: the creation of kinetic energy resulting based on the overall velocity gradients, production of kinetic energy due to buoyancy, and the role of fluctuating dilatation in turbulence in compressible flow in contributing to the average dissipation rate, respectively. C_2 and $C_{1\epsilon}$ have fixed data, while σ_k and σ_ϵ denote the Prandtl numbers under turbulent flow conditions in accordance with k and ϵ, correspondingly. In addition, S_k and S_ϵ represent source terms that are determined by the user. The eddy viscosity can may solve as follows [22]:

$$\mu_t = \rho C_\mu \frac{k^2}{\epsilon} \tag{13}$$

$$C_\mu = \frac{1}{A_0 + A_s\frac{kU^*}{\epsilon}} \tag{14}$$

$$U^* \equiv \sqrt{S_{IJ}S_{IJ} + \tilde{\Omega}_{IJ}\tilde{\Omega}_{IJ}} \tag{15}$$

$$\begin{aligned}\tilde{\Omega}_{IJ} &= \Omega_{ij} - 2\epsilon_{ijk}\omega_k \\ \Omega_{ij} &= \overline{\Omega_{ij}} - \epsilon_{ijk}\omega_k\end{aligned} \tag{16}$$

in which, $\overline{\Omega_{ij}}$ corresponds to the average rotational rate tensor as observed in a reference frame that rotates at a speed of ω_k. A_0 and A_S were utilized as model constants as follows [22]:

$$A_0 = 4.04,\ A_S = \sqrt{6}\cos\phi \tag{17}$$

$$\phi = \frac{1}{3}\cos^{-1}\left(\sqrt{6}W\right)\ W = \frac{S_{ij}S_{jk}S_{ki}}{\tilde{S}^3}\ \tilde{S} = \sqrt{S_{ij}S_{IJ}}\ S_{ij} = \frac{1}{2}\left(\frac{\partial u_j}{\partial x_i} + \frac{\partial u_i}{\partial x_j}\right) \tag{18}$$

$$C_{1\epsilon} = 1.44,\ C_2 = 1.9,\ \sigma_k = 1.0,\ \sigma_\epsilon = 1.2 \tag{19}$$

Table 3. Variable parameters for DPHEX.

			Levels			
Variable	Symbol	Unit	First level	Second level	Third level	Fourth level
Fluid types for tube-side	A	–	Water-liquid	Ethylene-glycol	Engine-oil	Benzene-liquid
Flow mass rates for shell-side	B	kg/s	1.1	1.5	–	–

4. Statistical analysis

In order to perform CFD analysis, two different variables were considered. Each variable is used at different levels. Taguchi method was utilized to choose the effect on ΔT_{LM} and U_{shell} depending on the least number of analyzes. Taguchi technique employs the use of orthogonal arrays to efficiently test the effects of multiple parameters on a given outcome. Orthogonal arrays are specifically designed to minimize the number of experiments required while still providing sufficient information to identify the optimal parameter settings. Additionally, Taguchi method uses a statistical approach. This can help to minimize the impact of noise and variability in the data, further reducing the number of analyses required. In the study, two different variables were considered. Each variable was evaluated as consisting of three different levels. Thus, for the CFD analysis, nine different analyzes were achieved depending on the L8 orthogonal array. The variables in CFD designs are illustrated in Table 3.

The type of fluid passing through the inside tube is utilized as the first variable. The second variable is the flow mass ratios of the fluid passing through the shell. Water-liquid, ethylene-glycol, and engine-oil are all important fluids commonly used in double pipe heat exchangers due to their ability to transfer heat efficiently. Water-Liquid is a common choice for low temperature applications due to its high heat capacity and low cost, while Ethylene-Glycol is often used in higher temperature applications where freezing is a concern. Engine-Oil is used in heat exchangers for engine cooling systems, and is chosen for its ability to transfer heat while also lubricating engine components. To define the effect of these variables on the results and their optimum levels, S/N ratio analysis was used. Taguchi method is used S/N ratio analysis to optimize the variables. The aim of S/N ratio analysis is to identify the combination of variables that results in the highest quality output, while minimizing the impact of noise factors that can affect the output quality. In Taguchi method, the goal is to optimize the control factors that impact the response characteristic, in order to achieve the highest possible "larger is better" value. This is done by conducting analyses and analyzing the data to identify the optimal combination of control factors that will produce the desired response characteristic. In this context, the "Larger is Better" approach was used to define the highest ΔT_{LM} and U_{shell} in shell pipe. The equation for "Larger is Better" approach is given as follows [26]:

$$(S/N)_{LB} = -10.\log\left(n^{-1}\sum_{i=1}^{n}\left(y_i^2\right)^{-1}\right) \tag{20}$$

in which, n denotes the number of measurements or observations that have been made for the response variable. Also, yi expresses the observed data of the response for the i^{th} measurement or observation. ANOVA was utilized to define the impact level and influence rate of variable on the results obtained. ANOVA is an important statistical method used to analyze differences between means in two or more groups.

5. Results and discussions

In this article, the impacts of different fluids passing through the inner tube and the flow mass ratio passing through the outer tube on ΔT_{LM} and U_{shell} in a DPHEX were investigated using numerical and statistical methods. Obtained CFD results were converted to S/N ratio values.

Table 4. CFD and S/N ratio data.

		Variables		Results			
Test	Code	A	B	Log-mean temperature ΔT_{LM}, (K)	S/N ratio η (dB)	Heat transfer coefficient U_{Shell}, (W/m^2-K)	S/N ratio η (dB)
1	A_1B_1	Water-liquid	1.1 kg/s	37.83056	31.5569	547.9410	54.7747
2	A_1B_2	Water-liquid	1.5 kg/s	38.02903	31.6023	659.0679	56.3786
3	A_2B_1	Ethylene-glycol	1.1 kg/s	40.98167	32.2518	201.0478	46.0660
4	A_2B_2	Ethylene-glycol	1.5 kg/s	41.17927	32.2936	231.0205	47.2730
5	A_3B_1	Engine-oil	1.1 kg/s	39.12347	31.8487	179.8897	45.1001
6	A_3B_2	Engine-oil	1.5 kg/s	39.69172	31.9740	108.6498	40.7206
7	A_4B_1	Benzene-liquid	1.1 kg/s	36.50604	31.2473	382.0711	51.6429
8	A_4B_2	Benzene-liquid	1.5 kg/s	36.62928	31.2766	450.2912	53.0699
Overall mean ($\bar{T}_m$)				38.74638		344.9974	

Calculated CFD and S/N ratio results in accordance with Taguchi L9 orthogonal array are demonstrated in Table 4.

The overall ΔT_{LM} is 38.74638, which indicates that the overall temperature change among the hot and cold liquids is close to 39 °C. Also, U_{shell} of DPHEX is calculated to be 344.9974 W/m^2-K. CFD results for temperature in Table 4 were presented in Figures 2–9.

6. Analysis of optimal levels

ANOVA was employed to identify the effective variables and their percent contribution rates on ΔT_{LM} and U_{shell}. ANOVA was utilized as a statistical technique to evaluate the variation levels between different data groups and identify the variables that have the most significant influence on the response variable of interest. ANOVA was implemented using Minitab statistical program at 95% confidence level and calculated outcomes are listed in Table 5.

According to the results in Table 5, the variables with the greatest impact on ΔT_{LM} were determined as fluid type with 99.09% effect rate and flow mass rate with 0.65% effect rate, respectively. The variables exerting the greatest influence on U_{shell} were calculated as fluid type with 95.73% effect rate and flow mass rate with 0.89% effect rate, respectively. The fluid type has a significant effect on ΔT_{LM} and U_{shell}, as the P value is calculated to be less than 0.05. However, P value indications that flow mass rate does not have a major impact for both outcomes. Based on these results, the flow mass rate is an insignificant variable and may not be taken into account in determining the optimum results, as it has a low level of importance. To observe to effects of fluids types and flow mass rates on ΔT_{LM} and U_{shell}, the study was conducted using a method called L8 orthogonal array, which involves two control factors. The average values of ΔT_{LM} and U_{shell} were determined for each fluid type and flow mass rate at three different levels. These values were compared to the S/N ratios to determine the overall impact of fluid types and flow mass rates on ΔT_{LM} and U_{shell}. The results for S/N ratios and means were presented in Table 6.

Table 6 shows the ideal fluid type and flow mass ratio for achieving optimal levels of ΔT_{LM} and U_{shell}. The second levels of the fluid type and the flow mass rate were considered as the ideal levels for ΔT_{LM}. In addition, the fluid type at the first level and the flow mass rate at the second level were found as the optimal levels for U_{shell}.

7. Impacts of variables on outputs

The impact and ideal ranges of fluid type and flow mass rate on ΔT_{LM} and U_{shell} were investigated using S/N ratio analysis. To realize the impacts of fluid type and flow mass rate on the responses, and the average CFD values obtained for each level of all variables were computed and

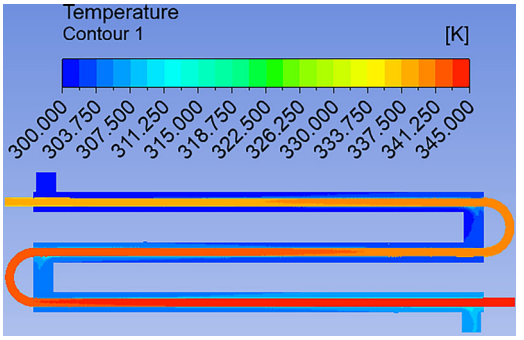

Figure 2. Temperature counter for A_1B_1.

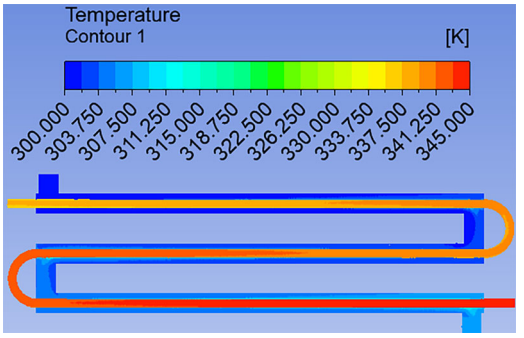

Figure 3. Temperature counter for A_1B_2.

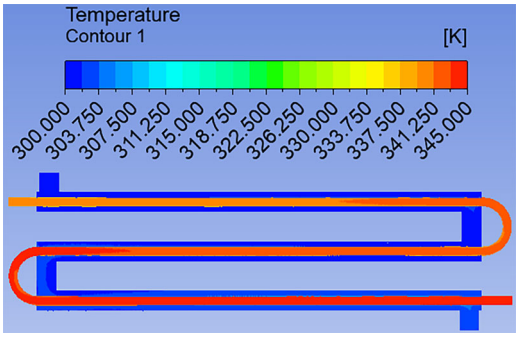

Figure 4. Temperature counter for A_2B_1.

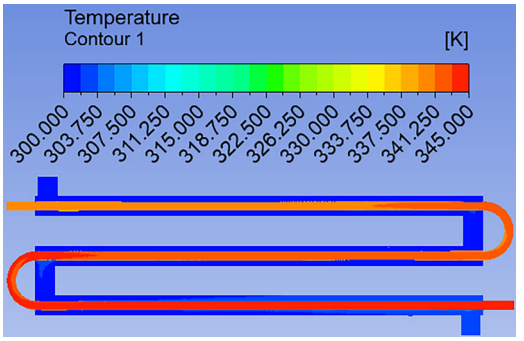

Figure 5. Temperature counter for A_2B_2.

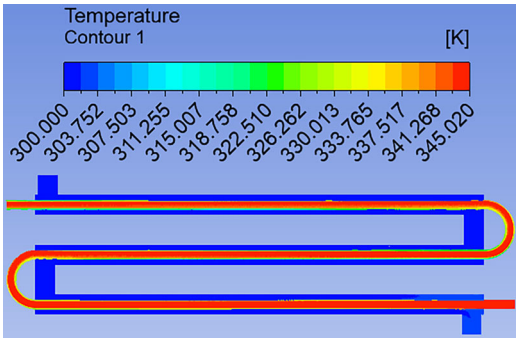

Figure 6. Temperature counter for A_3B_1.

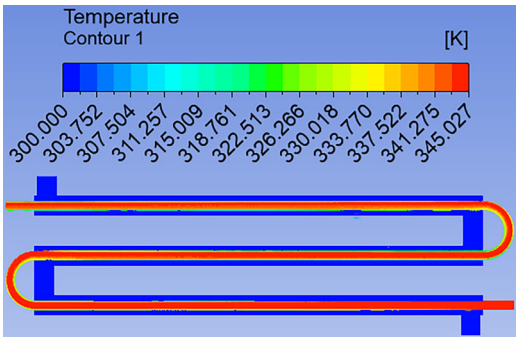

Figure 7. Temperature counter for A_3B_2.

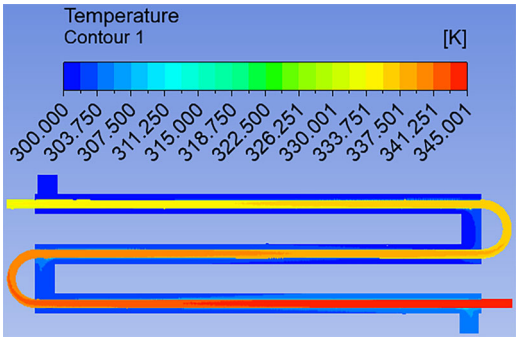

Figure 8. Temperature counter for A_4B_1.

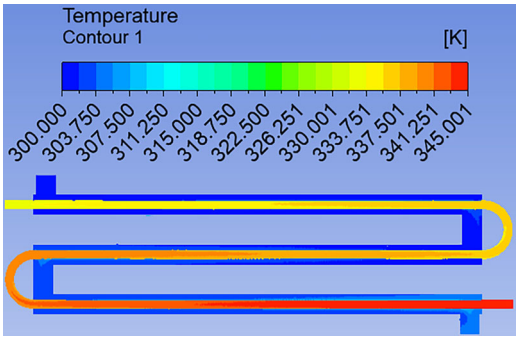

Figure 9. Temperature counter for A_4B_2.

plotted to create graphs. The graphs representing ΔT_{LM} and U_{shell} are observed in Figure 10 and Figure 11, respectively.

According to Figure 10, the highest ΔT_{LM} values are achieved by using ethylene-glycol, engine-oil, water-liquid, and benzene-liquid, respectively. This determination and this observation may be attributed to thermal characteristics for fluids. Each liquid has different thermal properties relative to each other. These thermal properties cause a temperature change at the inlet and outlet of the fluid passing through pipes in DPHEX. Occurred temperature differences cause different

Table 5. ANOVA results for ΔT_{LM} and U_{shell}.

	Log-mean temperature difference, ΔT_{LM}						Heat transfer coefficient, U_{shell}				
Source	DF	Seq SS	Adj MS	F	P	% Effect	Seq SS	Adj MS	F	P	% Effect
A	3	22.5976	7.5325	374.03	0	99.09	257632	85877	28.30	0.011	95.73
B	1	0.1478	0.1478	7.34	0.073	0.65	2383	2383	0.79	0.441	0.89
Error	3	0.0604	0.0201			0.26	9105	3035			3.38
Total	7	22.8059				100	269121				100
	R-Sq = 99.74% and R-Sq(adj) = 99.38%						R-Sq = 96.62% and R-Sq(adj) = 92.11%				

Table 6. Response table for ΔT_{LM} and U_{shell}.

	Log-mean temperature difference, ΔT_{LM}				Heat transfer coefficient U_{shell}			
	S/N ratio (dB)		Means (K)		S/N ratio (dB)		Means (W/m^2-K)	
Level	A	B	A	B	A	B	A	B
1	31.58	31.73	37.93	38.61	55.58	49.40	603.50	327.70
2	32.27	31.79	41.08	38.88	46.67	49.36	216.00	362.30
3	31.91		39.41		42.91		144.30	
4	31.26		36.57		52.36		416.20	
Delta	1.01	0.06	4.51	0.27	12.67	0.04	459.20	34.50
Rank	1	2	1	2	1	2	1	2

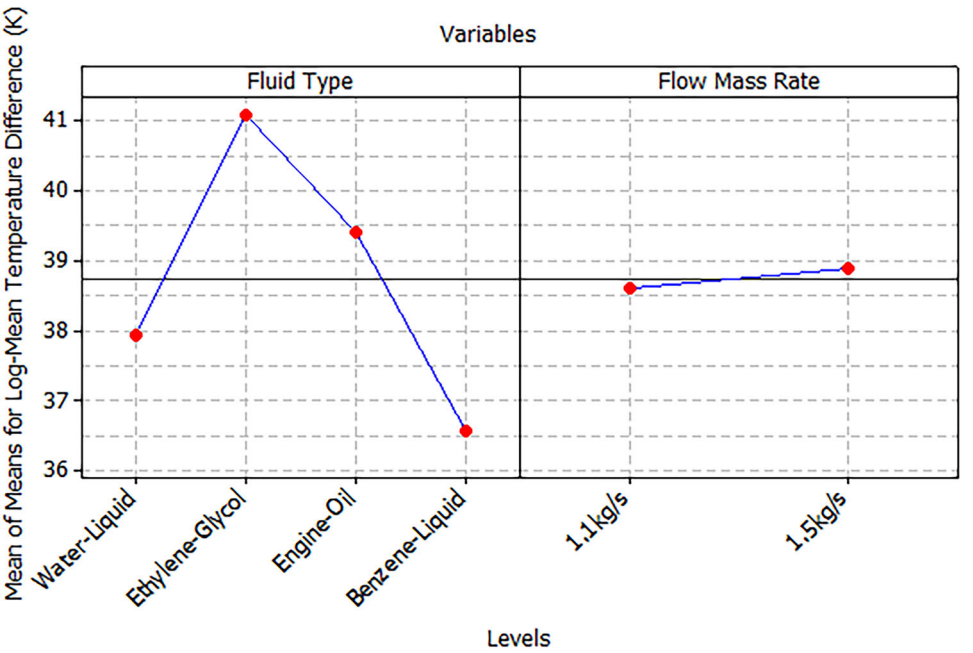

Figure 10. Main impacts on log-mean temperature difference.

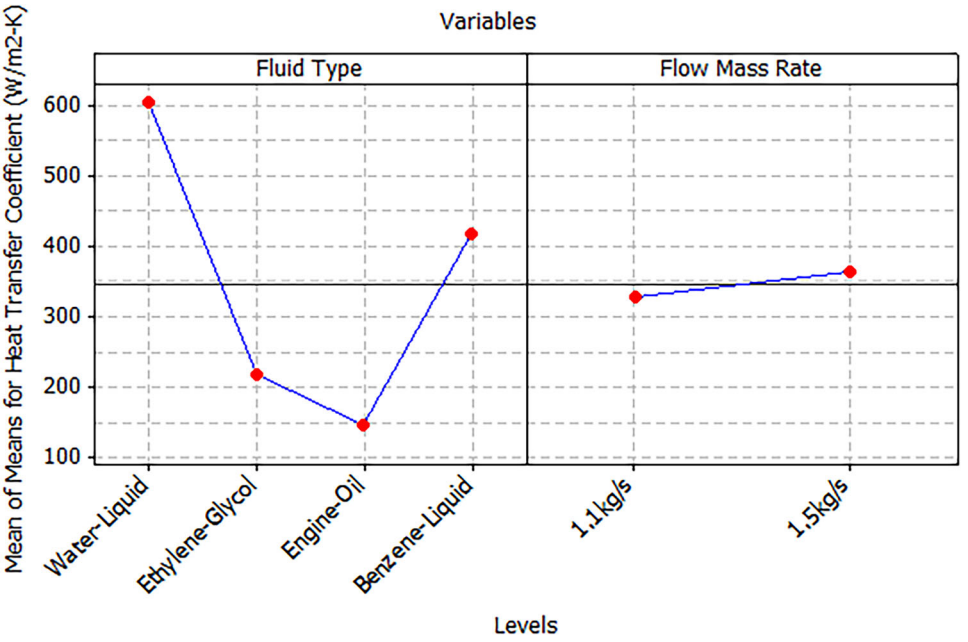

Figure 11. Main impacts on heat transfer coefficient.

ΔT_{LM}. Figure 11 demonstrations that the highest heat transfer coefficient values are achieved by using water-liquid and benzene-liquid, followed by ethylene-glycol and engine-oil. This may be because ethylene-glycol and water-liquid have higher thermal conductivity and specific heat capacity than engine-oil and benzene. The rise in the flow mass rate from 1.1 kg/s to 1.5 kg/s causes a rise in ΔT_{LM} and U_{shell}. The increase in flow mass rate can cause a higher fluid velocity, which in turn increases the rate of heat transfer. This is because higher flow rate causes an increase for Reynolds number, which is a dimensionless parameter that characterizes the flow regime. As the fluid velocity increases, the flow becomes more turbulent, which enhances heat transfer by increasing the mixing and promoting the formation of eddies and vortices that facilitate the transfer of heat from the hot surface to the fluid. The increase in ΔT_{LM} can be also related to the increase in flow mass rate. ΔT_{LM} is a measure of the temperature gradient among the hot and cold fluids, which drives the heat transfer process. The higher flow mass rate causes a greater rate for fluid flow. It was also supported by another study that the increase in fluid velocity directly affected the temperature change [27].

8. Estimation of optimal responses

To estimate ΔT_{LM} and U_{shell} of a DPHEX at optimal levels, it was necessary to consider the significant levels of variables such as fluid type in the inner tube and flow mass rate in the shell, using a significance level of $p < 0.05$. These determinations were made through an ANOVA performed at the 95% confidence level. Based on the results of the ANOVA, it was found that the second level of flow mass rate are the optimal values for both ΔT_{LM} and U_{shell}. In addition, the first level of the fluid type for U_{shell} and the second level of ΔT_{LM} were considered as the optimal levels. The estimated optimum results can be calculated with the following equation [26]:

$$\mu_k = \overline{A_k} + \overline{B_k} - \overline{T_m} \tag{21}$$

where, $\overline{T_m}$ is the overall mean for ΔT_{LM} =38.74638 and U_{shell} = 344.9974, respectively. $\overline{A_k}$ and $\overline{B_k}$ are the ideal ranks of the fluid type and the flow mass rate for DPHEX, respectively. $\overline{A_2}$ = 41.08

Table 7. Comparison of CFD and predicted results.

Combination	Outputs	CFD result (K)	Predicted result (W/m^2-K)	Difference
A_2B_2	Log-mean temperature difference	41.17927	41.2136	0.08 %
A_1B_2	Heat transfer coefficient	659.0679	620.8026	5.81 %

and $\overline{B_2}$ = 38.88 refer to the average ΔT_{LM} for fluid type and flow mass rate at the second levels, respectively. $\overline{A_1}$ = 603.50 is U_{shell} value at the first level for the fluid type . $\overline{B_2}$ = 362.30 is U_{shell} for flow mass rate at the second level. Substituting CFD values corresponding to these terms, $\mu_{\Delta T_{LM}}$ = 41.2136 K and μ_U = 620.8026 W/m^2-K are calculated. The differences between ΔT_{LM} and U_{shell} obtained depending on the estimation and CFD result were organized in Table 7.

9. Conclusions

In the study, CFD and statistical analysis of the impacts of fluid type and flow mass rate on ΔT_{LM} and U_{shell} in DPHEX were performed. CFD calculations were carried out using ANSYS Fluent software. Numerical investigation was conducted utilizing Taguchi L8 orthogonal array with two variables. Water-liquid, ethylene-glycol, engine-oil, and benzene-liquid were used as fluid types. The levels of flow mass rates were utilized as 1.1 kg/s and 1.5 kg/s. To decide the ideal levels of variables and variable impacts on ΔT_{LM} and U_{shell} in DPHEX, the analysis of S/N ratio was employed. ANOVA were utilized to identify the most effective variables and their contribution rates. The study's findings can be summarized as follows:

- The highest log-mean temperature differences are obtained by using ethylene-glycol, engine-oil, water-liquid, and benzene-liquid, respectively.
- The maximum heat transfer coefficient is found utilizing water-liquid, benzene-liquid, ethylene-glycol, and engine-oil, respectively.
- As the flow mass rate rises from 1.1 kg/s to 1.5 kg/s, both the log-mean temperature difference in DPHEX and the heat transfer coefficient for shell increase correspondingly.
- According to ANOVA results at a 95% confidence level, fluid type was found to be a significant factor in both the log-mean temperature difference in DPHEX and the heat transfer coefficient for shell.
- The most efficient variables on the log-mean temperature difference in DPHEX were found as fluid type with 99.09% impact and flow mass rate with 0.65% impact, respectively.
- The most meaningful variables on the heat transfer coefficient for shell were calculated as fluid type with 95.73% influence and flow mass rate with 0.89% influence, respectively.
- The fluid type has a major effect on the log-mean temperature difference in DPHEX and the heat transfer coefficient for shell due to F-test in ANOVA.
- The variables with optimal levels for the log-mean temperature difference in DPHEX and the heat transfer coefficient for shell are A_2B_2 and A_1B_2, respectively.
- The difference between the estimated and CFD results for the log-mean temperature difference in DPHEX was calculated as 0.08%, while the difference for the heat transfer coefficient for shell was determined as 5.81%.

ORCID

Savaş Evran http://orcid.org/0000-0002-7512-5997
Mustafa Kurt http://orcid.org/0000-0001-8714-977X

References

[1] P. C. Mukesh Kumar and M. Chandrasekar, "CFD analysis on heat and flow characteristics of double helically coiled tube heat exchanger handling MWCNT/water nanofluids," *Heliyon*, vol. 5, no. 7, pp. e02030, 2019. DOI: 10.1016/j.heliyon.2019.e02030.

[2] S. M. Shahril, G. A. Quadir, N. A. M. Amin and I. A. Badruddin, "Thermo hydraulic performance analysis of a shell-and-double concentric tube heat exchanger using CFD," *Int. J. Heat Mass Transfer*, vol. 105, pp. 781–798, 2017. DOI: 10.1016/j.ijheatmasstransfer.2016.10.021.

[3] D. Thondiyil and S. Kizhakke Kodakkattu, "Optimization of a shell and tube heat exchanger with staggered baffles using Taguchi method," *Mater. Today*, vol. 46, pp. 9983–9988, 2021. DOI: 10.1016/j.matpr.2021.04.092.

[4] M. Vivekanandan, R. Venkatesh, R. Periyasamy, S. Mohankumar and L. Devakumar, "Experimental and CFD investigation of helical coil heat exchanger with flower baffle," *Mater. Today*, vol. 37, pp. 2174–2182, 2021. DOI: 10.1016/j.matpr.2020.07.642.

[5] H. Wang, Y-w Liu, P. Yang, R-j Wu and Y-l He, "Parametric study and optimization of H-type finned tube heat exchangers using Taguchi method," *Appl. Therm. Eng.*, vol. 103, pp. 128–138, 2016. DOI: 10.1016/j.applthermaleng.2016.03.033.

[6] D. Zheng, J. Du, W. Wang, J. J. Klemeš, J. Wang and B. Sundén, "Analysis of thermal efficiency of a corrugated double-tube heat exchanger with nanofluids," *Energy*, vol. 256, pp. 124522, 2022. DOI: 10.1016/j.energy.2022.124522.

[7] X. Li, L. Wang, R. Feng, Z. Wang, S. Liu and D. Zhu, "Study on shell side heat transport enhancement of double tube heat exchangers by twisted oval tubes," *Int. Commun. Heat Mass Transf.*, vol. 124, pp. 105273, 2021. DOI: 10.1016/j.icheatmasstransfer.2021.105273.

[8] T. Rajeh, B. H. Al-Kbodi, Y. Li, J. Zhao and Y. Zhang, "Modeling and techno-economic comparison of two types of coaxial with double U-tube ground heat exchangers," *Appl. Therm. Eng.*, vol. 225, pp. 120221, 2023. DOI: 10.1016/j.applthermaleng.2023.120221.

[9] C. Luo and K. Song, "Thermal performance enhancement of a double-tube heat exchanger with novel twisted annulus formed by counter-twisted oval tubes," *Int. J. Therm. Sci.*, vol. 164, pp. 106892, 2021. DOI: 10.1016/j.ijthermalsci.2021.106892.

[10] C. Qi, T. Luo, M. Liu, F. Fan and Y. Yan, "Experimental study on the flow and heat transfer characteristics of nanofluids in double-tube heat exchangers based on thermal efficiency assessment," *Energy Convers. Manag.*, vol. 197, pp. 111877, 2019. DOI: 10.1016/j.enconman.2019.111877.

[11] J. D. Moya-Rico, A. E. Molina, J. F. Belmonte, J. I. Córcoles Tendero and J. A. Almendros-Ibáñez, "Experimental characterization of a double tube heat exchanger with inserted twisted tape elements," *Appl. Therm. Eng.*, vol. 174, pp. 115234, 2020. DOI: 10.1016/j.applthermaleng.2020.115234.

[12] A. J. Baker, C.-X. Lin, J. A. Orzechowski and C. Gordon, "Fully Coupled 3-D Conjugate Heat Transfer Algorithm for Borehole Heat Exchanger Performance Prediction," *Numer. Heat Transf. B*, vol. 60, no. 3, pp. 147–167, 2011. DOI: 10.1080/10407790.2011.601185.

[13] P. Asinari, "Finite-volume and finite-element hybrid technique for the calculation of complex heat exchangers by semiexplicit method for wall temperature linked equations (SEWTLE)," *Numerical Numer. Heat Transf. B*, vol. 45, no. 3, pp. 221–247, 2004. DOI: 10.1080/10407790490268995.

[14] A. Khanlari, A. Sözen and H. İ. Variyenli, "Simulation and experimental analysis of heat transfer characteristics in the plate type heat exchangers using TiO2/water nanofluid," *HFF*, vol. 29, no. 4, pp. 1343–1362, 2019. DOI: 10.1108/HFF-05-2018-0191.

[15] S. Kumar and K. Murugesan, "Optimization of geothermal interaction of a double U-tube borehole heat exchanger for space heating and cooling applications using Taguchi method and utility concept," *Geothermics*, vol. 83, pp. 101723, 2020. DOI: 10.1016/j.geothermics.2019.101723.

[16] Y. Feng, R. Xu, Y. Cao, X. Wu, C. Liang and L. Zhang, "Optimization of H-type finned tube heat exchangers with combinations of longitudinal vortex generator, dimples/protrusions and grooves by Taguchi method," *Int. Commun. Heat Mass Transf.*, vol. 143, pp. 106709, 2023. DOI: 10.1016/j.icheatmasstransfer.2023.106709.

[17] J. Jiang, et al., "Evaluation of the long-term performance of the deep U-type borehole heat exchanger on different geological parameters using the Taguchi method," *J. Build. Eng.*, vol. 59, pp. 105122, 2022. DOI: 10.1016/j.jobe.2022.105122.

[18] S. Chamoli, P. Yu and A. Kumar, "Multi-response optimization of geometric and flow parameters in a heat exchanger tube with perforated disk inserts by Taguchi grey relational analysis," *Appl. Therm. Eng.*, vol. 103, pp. 1339–1350, 2016. DOI: 10.1016/j.applthermaleng.2016.04.166.

[19] M. Ghalambaz, et al., "Melting process of the nano-enhanced phase change material (NePCM) in an optimized design of shell and tube thermal energy storage (TES): taguchi optimization approach," *Appl. Therm. Eng.*, vol. 193, pp. 116945, 2021. DOI: 10.1016/j.applthermaleng.2021.116945.

[20] N. Celik, G. Pusat and E. Turgut, "Application of Taguchi method and grey relational analysis on a turbulated heat exchanger," *Int. J. Therm. Sci.*, vol. 124, pp. 85–97, 2018. DOI: 10.1016/j.ijthermalsci.2017.10.007.
[21] ANSYS., "Fluent Software Material Database, Canonsburg, PA: ANSYS Inc." 2021.
[22] ANSYS., "Ansys Fluent 12.0 theory guide." ANSYS Inc., Canonsburg, PA. 2009.
[23] S. J. M. Cartaxo and F. A. N. Fernandes, "Counterflow logarithmic mean temperature difference is actually the upper bound: A demonstration," *Appl. Therm. Eng.*, vol. 31, no. 6-7, pp. 1172–1175, 2011. DOI: 10.1016/j.applthermaleng.2010.12.015.
[24] R. Hosseini, A. Hosseini-Ghaffar and M. Soltani, "Experimental determination of shell side heat transfer coefficient and pressure drop for an oil cooler shell-and-tube heat exchanger with three different tube bundles," *Appl. Therm. Eng.*, vol. 27, no. 5-6, pp. 1001–1008, 2007. DOI: 10.1016/j.applthermaleng.2006.07.023.
[25] B.-H. Chun, H. U. Kang and S. H. Kim, "Effect of alumina nanoparticles in the fluid on heat transfer in double-pipe heat exchanger system," *Korean J. Chem. Eng.*, vol. 25, no. 5, pp. 966–971, 2008. DOI: 10.1007/s11814-008-0156-5.
[26] P. J. Ross, *Taguchi techniques for quality engineering*, 2nd ed. New York, NY, USA: McGraw-Hill International Editions, 1996.
[27] S. Evran and M. Kurt, "CFD and statistical analysis of flow mass ratios on temperature and pressure drops of double pipe heat exchanger," *Int. J. Low-Carbon Technol.*, vol. 18, pp. 771–780, 2023. DOI: 10.1093/ijlct/ctad056.